Journal of Sound and Vibration (1998) **209**(4), 635–650

ACTIVE VIBRATION CONTROL OF COMPOSITE BEAMS WITH PIEZOELECTRICS: A FINITE ELEMENT MODEL WITH THIRD ORDER THEORY

X. Q. Peng, K. Y. Lam and G. R. Liu

Department of Mechanical and Production Engineering, *National University of Singapore*, 10 *Kent Ridge Crescent*, *Singapore* 119260

(*Received* 30 *September* 1996, *and in final form* 28 *July* 1997)

A finite element model based on third order laminate theory is developed for the active position control and vibration control of composite beams with distributed peizoelectric sensors and actuators. The direct peizoelectric equation is used to calculate the total charge created by the strains on the sensor electrodes; and the actuators provide a damping effect on the composite beam by coupling a negative velocity feedback control algorithm in a closed control loop. The shape control and active vibration suppression of a cantilever composite beam are performed to verify the proposed model. A modal superposition technique and the Newmark-β method are used in the numerical analysis to compute the dynamic response of composite beams. Finally, the effects of the number and locations of the sensors/actuators on the control system are also investigated.

1. INTRODUCTION

Usually, satellites and other large-scale space structures have low flexural rigidity and are lightly damped due to the small material damping and the lack of other forms of damping in the space. This may lead to destructive large amplitude vibration and long vibration decay times and thus result in fatigue, instability and poor operation of the structures. Attempts at solving these problems have recently stimulated extensive research into smart structures and systems.

A smart structure can be defined as a structure or structural component with bonded or embedded sensors and actuators as well as an associated control system, which enable the structure to respond simultaneously to external stimuli exerted on it and then suppress undesired effects or enhance desired effects. This technique improves the performance of existing structures and opens opportunities for radical changes in the design of adaptive structures, high performance structures, high precision systems, etc. Moreover, recent advances in design and manufacturing technologies of piezoelectric sensors and actuators have enhanced the efficiency of smart systems.

Piezoelectric materials, such as lead zirconate titanate (PZT), have coupled mechanical and electrical properties. They exhibit mechanical deformation when subjected to an applied electric field, which is called the converse piezoelectric effect. They also generate a voltage or charge when subjected to a force or deformation, which is termed as the direct piezoelectric effect. Bonding or embedding piezoelectric patches in a structure can act as sensors to monitor or as actuators to control the response of the structure. However, before piezoelectric sensors and actuators can be incorporated into a smart system, the mechanical interaction between the piezoelectrics and the underlying structure must be well understood. Several investigators have recently developed analytical and numerical linear

0022–460X/98/040635 + 15 $25.00/0/sv971249

or non-linear models for the responses of integrated piezoelectric structures [1–9]. These models offer a platform to explore the active vibration control in smart structures.

Bailey and Hubbard [1] have successfully used piezoelectric sensors and actuators in the vibration control of isotropic cantilever beams. Based on the classical laminated plate theory, Lee [7] presented a mathematical model for distributed sensors and actuators and used this model in the vibration control of laminated structures. Shen [10] developed an analytical model for the prediction and control of bending and torsional vibration response of a composite beam with piezoelectric damping treatments. Shi and Atluri [11] presented a scheme for active control of non-linear vibration of space structures, wherein each member was modelled as a beam-column. Additionally, by integrating certain feedback control loops, some finite element models were also developed for the active vibration control or suppression of structures with distributed piezoelectrics [12–18].

Tzou [12] proposed a general theory on the distributed sensing and active vibration suppression using piezoelectrics and then developed an equivalent finite element formulation for elastic or flexible manipulators. Tzou and Tseng [13] also presented a piezoelectric finite element model with internal degrees of freedom for modelling the flexibility and versatility, and used it in the analysis of the measurement/control of distributed parameter systems. Ha *et al*. [14] developed a three-dimensional brick element to model the dynamic and static response of laminated composites containing distributed piezoelectrics, and then studied the active response control of the integrated structures by coupling simple control algorithms in a closed loop. Based on the classical theory, Hwang and Park [15] studied the vibration control of a laminated plate using a four-node quadrilateral element with one electrical degree of freedom. Chandrashekhara *et al*. [16, 17] developed a piezoelectric finite element model based on a first order shear deformation theory and analyzed the thermally induced vibration suppression of laminated plates with piezoelectric sensors and actuators. Shieh [18] proposed a finite element model for multi-axially active laminated piezoelectric beam elements capable of spontaneously sensing/actuating all axial extension, biaxial bending and torsional twisting of beam deformation.

However, the accuracy and efficiency of active vibration control or suppression models depend on the perfection of understanding the mechanical interaction between the piezoelectrics and the underlying structure. The classical theory used to model the beam deformation is based on the Kirchhoff–Love assumption and thus neglects the transverse shear deformation effects; on the other hand, the main drawback of the shear deformation theory is that it needs a shear correction factor, which is very difficult to determine especially for arbitrarily laminated composite structures with piezoelectric layers. To overcome the above-mentioned drawbacks, Reddy *et al*. [4–6] developed a third order laminate theory, which accommodates quadratic variation of transverse shear strains and eliminates the transverse shear stresses on the top and bottom of a laminated composite structure. Thus no shear correction factor is needed in the third order theory.

In the present work, a finite element model based on third order laminate theory is developed for the active vibration control of composite beams with distributed piezoelectric sensors and actuators. A simple negative velocity feedback control algorithm is coupled in a close control loop. The shape control and active vibration suppression of a cantilever composite beam are performed to demonstrate the presented model. A modal superposition technique and the Newmark-β method are used to calculate the dynamic response. Finally, the effects of the number and locations of the sensors/actuators on the control system are also evaluated.

2. PIEZOELECTRIC EQUATIONS

It is assumed that the thermal effect is not considered in the analysis. The linear piezoelectric coupling between the elastic field and the electric field can be expressed by the direct and the converse piezoelectric equations respectively [19]:

$$\{D\} = [e]\{\varepsilon\} + [\varepsilon]\{E\}, \qquad \{\sigma\} = [Q]\{\varepsilon\} - [e]^{\mathrm{T}}\{E\} \tag{1, 2}$$

where $\{\sigma\}$ is the stress vector, $[Q]$ is the elastic stiffness matrix, $\{\varepsilon\}$ is the strain vector, $[e]$ is the piezoelectric constant matrix, $[e]^{\mathrm{T}}$ is the transpose of $[e]$, $\{E\}$ is the electric field vector, $\{D\}$ is the electric displacement vector and $[\varepsilon]$ is the permittivity matrix. The superscript "T" denotes the transpose of a vector or matrix.

Assuming that a laminated beam consists of a number of layers (including the piezoelectric layers) and each layer possesses a plane of material symmetrically parallel to the x–y plane, the constitutive equations for the kth layer can be written as

$$\begin{Bmatrix} D_1 \\ D_3 \end{Bmatrix}_k = \begin{bmatrix} 0 & e_{15} \\ e_{31} & 0 \end{bmatrix}_k \begin{Bmatrix} \varepsilon_1 \\ \varepsilon_5 \end{Bmatrix}_k + \begin{bmatrix} \varepsilon_{11} & 0 \\ 0 & \varepsilon_{33} \end{bmatrix}_k \begin{Bmatrix} E_1 \\ E_3 \end{Bmatrix}_k, \tag{3}$$

$$\begin{Bmatrix} \sigma_1 \\ \sigma_5 \end{Bmatrix}_k = \begin{bmatrix} Q_{11} & 0 \\ 0 & Q_{55} \end{bmatrix}_k \begin{Bmatrix} \varepsilon_1 \\ \varepsilon_5 \end{Bmatrix}_k - \begin{bmatrix} 0 & e_{31} \\ e_{15} & 0 \end{bmatrix}_k \begin{Bmatrix} E_1 \\ E_3 \end{Bmatrix}_k, \tag{4}$$

where the Q_{ii} are the reduced elastic constants of the kth layer:

$$Q_{11} = \frac{E_{11}}{1 - v_{12}\, v_{21}}, \qquad Q_{55} = G_{13},$$

where E_{11} is the Young's modulus and G_{13} is the shear modulus.

The piezoelectric constant matrix $[e]$ can be expressed in terms of the piezoelectric strain constant matrix $[d]$ as

$$[e] = [d]\,[Q], \tag{5}$$

where

$$[d] = \begin{bmatrix} 0 & d_{15} \\ d_{31} & 0 \end{bmatrix}. \tag{6}$$

3. FINITE ELEMENT MODEL

3.1. DISPLACEMENT FIELD OF THE THIRD ORDER THEORY

The displacement field based on the third order beam theory of Reddy [6] is given by

$$u(x, z, t) = u_0(x, t) + z\phi_x(x, t) - \alpha z^3\left(\phi_x + \frac{\partial w_0}{\partial x}\right), \tag{7}$$

$$w(x, z, t) = w_0(x, t), \tag{8}$$

where u and w are the displacement components in the x and z directions respectively, u_0 and w_0 are the midplane displacements and ϕ_x is the bending rotation of x-axis, $\alpha = 4/(3h^2)$ and h is the total thickness of the beam.

The displacement functions are approximated over each finite element by

$$u_0(x, t) = \sum_{i=1}^{2} u_i(t)\psi_i(x), \tag{9}$$

$$\phi_x(x, t) = \sum_{i=1}^{2} \phi_i(t)\psi_i(x), \tag{10}$$

$$w_0(x, t) = \sum_{i=1}^{4} \Delta_i(t)\varphi_i(x), \tag{11}$$

where the ψ_i are the linear Lagrangian interpolation polynomials and the φ_i are the cubic Hermit interpolation polynomials. Δ_1 and Δ_3 represent nodal values of w_0, whereas Δ_2 and Δ_4 represent nodal values of $\partial w_0/\partial x$.

We define

$$\{u\} = \{u \quad w\}^{\mathrm{T}}, \qquad \{\bar{u}\} = \{u_1 \quad \phi_1 \quad \Delta_1 \quad \Delta_2 \quad u_2 \quad \phi_2 \quad \Delta_3 \quad \Delta_4\}^{\mathrm{T}}.$$

Then equations (7) and (8) can also be expressed as

$$\{u\} = [N]\{\bar{u}\}, \tag{12}$$

where

$$[N] = \begin{bmatrix} \psi_1 & 0 \\ (z - \alpha z^3)\psi_1 & 0 \\ -\alpha z^3 \dfrac{\partial \varphi_1}{\partial x} & \varphi_1 \\ -\alpha z^3 \dfrac{\partial \varphi_2}{\partial x} & \varphi_2 \\ \psi_2 & 0 \\ (z - \alpha z^3)\psi_2 & 0 \\ -\alpha z^3 \dfrac{\partial \varphi_3}{\partial x} & \varphi_3 \\ -\alpha z^3 \dfrac{\partial \varphi_4}{\partial x} & \varphi_4 \end{bmatrix}^{\mathrm{T}}. \tag{13}$$

The strain–displacement relations are given by

$$\{\varepsilon\} = \begin{Bmatrix} \varepsilon_1 \\ \varepsilon_5 \end{Bmatrix} = [B]\{\bar{u}\}, \tag{14}$$

where

$$[B] = \begin{bmatrix} \dfrac{\partial \psi_1}{\partial x} & 0 \\ (z - \alpha z^3)\dfrac{\partial \psi_1}{\partial x} & (1 - 3\alpha z^2)\psi_1 \\ -\alpha z^3 \dfrac{\partial^2 \varphi_1}{\partial x^2} & (1 - 3\alpha z^2)\dfrac{\partial \varphi_1}{\partial x} \\ -\alpha z^3 \dfrac{\partial^2 \varphi_2}{\partial x^2} & (1 - 3\alpha z^2)\dfrac{\partial \varphi_2}{\partial x} \\ \dfrac{\partial \psi_2}{\partial x} & 0 \\ (z - \alpha z^3)\dfrac{\partial \psi_2}{\partial x} & (1 - 3\alpha z^2)\psi_2 \\ -\alpha z^3 \dfrac{\partial^2 \varphi_3}{\partial x^2} & (1 - 3\alpha z^2)\dfrac{\partial \varphi_3}{\partial x} \\ -\alpha z^3 \dfrac{\partial^2 \varphi_4}{\partial x^2} & (1 - 3\alpha z^2)\dfrac{\partial \varphi_4}{\partial x} \end{bmatrix}^{\mathrm{T}}. \tag{15}$$

3.2. DYNAMIC EQUATIONS

The dynamic equations of a piezoelectric structure can be derived by using Hamilton's principle:

$$\delta \int_{t_1}^{t_2} [T - U + W]\, \mathrm{d}t = 0, \tag{16}$$

where T is the kinetic energy, U is the strain energy, and W is the work done by the applied forces. Here the electric force due to the applied charge of the actuator is not considered.

The kinetic energy at the element level is defined as

$$T^e = \tfrac{1}{2} \int_{V_e} \rho \{\dot{u}\}^{\mathrm{T}} \{\dot{u}\}\, \mathrm{d}V, \tag{17}$$

where V_e is the volume of the beam element.

The strain energy can be written as

$$U^e = \tfrac{1}{2} \int_{V_e} \{\varepsilon\}^{\mathrm{T}} \{\sigma\}\, \mathrm{d}V. \tag{18}$$

The work done by the external forces is

$$W^e = \int_{V_e} \{u\}^{\mathrm{T}} \{f_b\}\, \mathrm{d}V + \int_{S_1} \{u\}^{\mathrm{T}} \{f_s\}\, \mathrm{d}S + \{u\}^{\mathrm{T}} \{f_c\}, \tag{19}$$

where $\{f_b\}$ is the body force, S_1 is the surface area of the beam element, $\{f_s\}$ is the surface force and $\{f_c\}$ is the concentrated load.

The electric field vector $\{E\}$ is defined by the electrical potential energy ϕ as

$$E = -\nabla \phi, \tag{20}$$

where ∇ denotes the gradient operator.

When an actuator layer with thickness h_A is applied a voltage V^e only in the thickness direction, the electric field vector $\{E\}$ can be expressed as

$$\{E\} = \{0 \quad V^e/h_A\}^{\mathrm{T}} = [0 \quad 1/h_A]^{\mathrm{T}} V^e = [B_v] V^e. \tag{21}$$

Substituting equations (17)–(19) into equation (16) and using equations (12), (14) and (21), the dynamic matrix equations can be written as

$$[M^e]\{\ddot{\bar{u}}\}^e + [K^e]\{\bar{u}\}^e = \{F\}^e + [K^e_{uv}] V^e, \tag{22}$$

where

$$[M^e] = \int_{V_e} \rho [N]^{\mathrm{T}} [N] \, \mathrm{d}V, \tag{23}$$

$$[K^e] = \int_{V_e} [B]^{\mathrm{T}} [Q] \, [B] \, \mathrm{d}V, \tag{24}$$

$$[K^e_{uv}] = \int_{V_e} [B]^{\mathrm{T}} [e]^{\mathrm{T}} [B_v] \, \mathrm{d}V, \tag{25}$$

$$\{F^e\} = \int_{V_e} [N]^{\mathrm{T}} \{f_b\} \, \mathrm{d}V + \int_{S_1} [N]^{\mathrm{T}} \{f_s\} \, \mathrm{d}S + [N]^{\mathrm{T}} \{f_c\}. \tag{26}$$

In order to include the damping effects, Rayleigh damping is assumed. Accordingly, equation (22) is modified as

$$[M^e]\{\ddot{\bar{u}}\}^e + [C^e]\{\dot{\bar{u}}\}^e + [K^e]\{\bar{u}\}^e = \{F\}^e + [K^e_{uv}\}] V^e, \tag{27}$$

where $[C^e]$ is the damping matrix, which is the form of

$$[C^e] = a[M^e] + b[K^e], \tag{28}$$

where a and b are constants that can be determined from experiments [20].

Assembling all the elemental equations gives the global dynamic equation

$$[\mathbf{M}]\{\ddot{\bar{\mathbf{u}}}\} + [\mathbf{C}]\{\dot{\bar{\mathbf{u}}}\} + [\mathbf{K}]\{\bar{\mathbf{u}}\} = \{\mathbf{F}\} + \{\mathbf{F}_{\mathrm{V}}\}, \tag{29}$$

where $\{\mathbf{F}\}$ is the external mechanical force vector and $\{\mathbf{F}_{\mathrm{V}}\}$ is the electrical force vector:

$$\{\mathbf{F}_{\mathrm{V}}\} = [\mathbf{K}_{\mathbf{uv}}]\{\mathbf{V}\}. \tag{30}$$

3.3. SENSOR EQUATION

Since no external electric field is applied to the sensor layer and as charge is collected only in the thickness direction, only the electric displacement D_3 is of interest and can be derived from equation (3) as

$$D_3 = e_{31} \varepsilon_1. \tag{31}$$

The total charge developed on the sensor surface is the spatial summation of all the point charges on the sensor layer. Hence, the closed circuit charge measured through the electrodes of a sensor patch in the kth layer is

$$q(t) = \tfrac{1}{2}\left[\int_{S_{2(z=z_k)}} D_3 \, \mathrm{d}S + \int_{S_{2(z=z_{k+1})}} D_3 \, \mathrm{d}S\right], \tag{32}$$

where S_2 is the effective surface electrode of the patch, which defines the integration domain where all the points are covered with surface electrode on both sides of the sensor lamina. In the present work, it is assumed that the whole piezoelectric lamina serves as the effective surface electrode.

Assuming that the sensor patch covers several elements, the total charge $q(t)$ can be written as follows:

$$q(t) = \sum_{j=1}^{N_s} \tfrac{1}{2}\left[\int_{S_j(z=z_k)} D_3 \, \mathrm{d}S + \int_{S_j(z=z_{k+1})} D_3 \, \mathrm{d}S\right]$$

$$= \sum_{j=1}^{N_s} \tfrac{1}{2}\left[\int_{S_j(z=z_k)} e_{31}\, \varepsilon_1 \, \mathrm{d}S + \int_{S_j(z=z_{k+1})} e_{31}\, \varepsilon_1 \, \mathrm{d}S\right], \tag{33}$$

where N_s is the number of elements, and S_j is the surface of the jth element.

Using equation (14), equation (33) can be rewritten as

$$q(t) = \sum_{j=1}^{N_s} \tfrac{1}{2}\left[\int_{S_j} ([B_1]_{(z=z_k)} + [B_1]_{(z=z_{k+1})}) e_{31} \, \mathrm{d}S\{\bar{u}_j\}\right], \tag{34}$$

where $[B_1]$ is the first row of $[B]$.

The current on the surface of a sensor can be expressed as

$$i(t) = \mathrm{d}q(t)/\mathrm{d}t. \tag{35}$$

When the piezoelectric sensors are used as strain rate sensors, the current can be converted into the open circuit sensor voltage output V_S by

$$V_S(t) = G_c\, i(t) = G_c \frac{\mathrm{d}q(t)}{\mathrm{d}t}, \tag{36}$$

where G_c is the gain of the current amplifier.

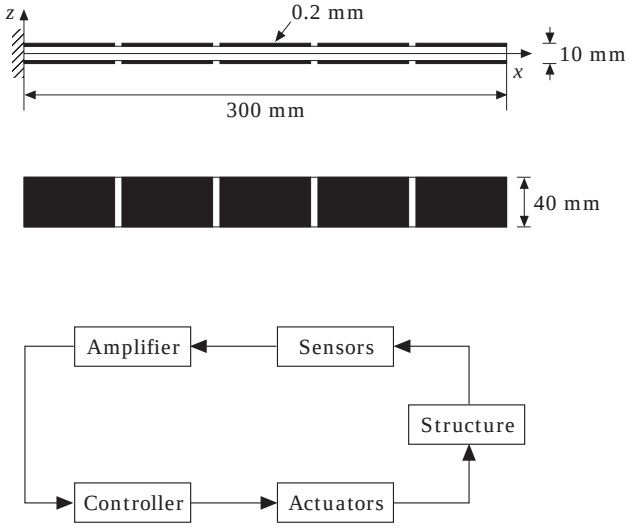

Figure 1. A cantilever composite beam with surface-bonded piezoelectric sensors and actuators.

3.4. ACTIVE CONTROL OF DAMPING

The distributed sensor generates a voltage when the structure is oscillating; and this signal is fed back into the distributed actuator using a control algorithm, as shown in Figure 1. The actuating voltage under a constant gain control algorithm can be expressed as

$$V^e = G_i V_S = G_i G_c \frac{\mathrm{d}q}{\mathrm{d}t}, \tag{37}$$

where G_i is the gain to provide feedback control.

Substituting equation (34) into equation (37) yields

$$V^e = G \sum_{j=1}^{N_s} [K_v^j]\{\ddot{\bar{u}}_j\}, \tag{38}$$

where

$$[K_v^j] = \tfrac{1}{2} \int_{S_j} ([B_1]_{(z=z_k)} + [B_1]_{(z=z_{k+1})}) e_{31} \, \mathrm{d}S, \tag{39}$$

$$G = G_i G_c. \tag{40}$$

Therefore, the system actuating voltages can be written as

$$\{\mathbf{V}\} = [\mathbf{G}]\,[\mathbf{K}_\mathbf{v}]\{\dot{\bar{\mathbf{u}}}\}, \tag{41}$$

where [**G**] is the control gain matrix.

In the feedback control, the electrical force vector $\{\mathbf{F}_\mathbf{v}\}$ can be regarded as a feedback force. Substituting equation (41) into equation (30) gives

$$\{\mathbf{F}_\mathbf{v}\} = [\mathbf{K}_\mathbf{uv}]\,[\mathbf{G}]\,[\mathbf{K}_\mathbf{v}]\{\dot{\bar{\mathbf{u}}}\}. \tag{42}$$

We define

$$[\mathbf{C}^*] = -[\mathbf{K}_\mathbf{uv}]\,[\mathbf{G}]\,[\mathbf{K}_\mathbf{v}]. \tag{43}$$

Thus, the system equation of motion equation (29) becomes

$$[\mathbf{M}]\{\ddot{\bar{\mathbf{u}}}\} + ([\mathbf{C}] + [\mathbf{C}^*])\{\dot{\bar{\mathbf{u}}}\} + [\mathbf{K}]\{\bar{\mathbf{u}}\} = \{\mathbf{F}\}. \tag{44}$$

As shown in equation (44), the voltage control algorithm equation (37) has a damping effect on the vibration suppression of a distributed system.

To obtain the dynamic response under a given external loading condition, a modal analysis is used, and the nodal displacement $\{\bar{\mathbf{u}}\}$ is represented by

$$\{\bar{\mathbf{u}}\} = [\mathbf{\Phi}]\{\mathbf{x}\}, \tag{45}$$

where $\{\mathbf{x}\}$ are referred to as the generalized displacements. [**Φ**] is the modal matrix and has the orthogonal property as follows:

$$[\mathbf{\Phi}]^\mathrm{T}[\mathbf{K}]\,[\mathbf{\Phi}] = [\mathbf{\Omega}^2], \qquad [\mathbf{\Phi}]^\mathrm{T}[\mathbf{M}]\,[\mathbf{\Phi}] = [\mathbf{I}], \tag{46, 47}$$

where $[\mathbf{\Omega}^2]$ is a diagonal matrix that stores the square of the natural frequencies ω_i.

Substituting equation (45) into equation (44), and then multiplying equation (44) by $[\mathbf{\Phi}]^\mathrm{T}$ yields

$$[\mathbf{\Phi}]^\mathrm{T}[\mathbf{M}]\,[\mathbf{\Phi}]\{\ddot{\mathbf{x}}\} + [\mathbf{\Phi}]^\mathrm{T}([\mathbf{C}] + [\mathbf{C}^*])\,[\mathbf{\Phi}]\{\dot{\mathbf{x}}\} + [\mathbf{\Phi}]^\mathrm{T}[\mathbf{K}]\,[\mathbf{\Phi}]\{\mathbf{x}\} = [\mathbf{\Phi}]^\mathrm{T}\{\mathbf{F}\}. \tag{48}$$

TABLE 1

Material properties PZT G1195N *piezoceramics and* T300/976 *graphite/epoxy composites*

	PZT	T300/976
Young's moduli (GPa)		
E_{11}	63·0	150·0
$E_{22} = E_{33}$	63·0	9.0
Poisson ratio		
$\nu_{12} = \nu_{13}$	0·3	0·3
ν_{23}	0·3	0·3
Shear moduli (GPa)		
$G_{12} = G_{13}$	24·2	7·10
G_{23}	24·2	2·50
Density, ρ (kg/mg^3):	7600	1600
Piezoelectric constants (m/V)		
$d_{31} = d_{32}$	254×10^{-12}	
Electrical permittivity (F/m)		
$\varepsilon_{11} = \varepsilon_{22}$	$15{\cdot}3 \times 10^{-9}$	
ε_{33}	$15{\cdot}0 \times 10^{-9}$	

Substituting equations (47) and (46) into equation (48) gives

$$\{\ddot{\mathbf{x}}\} + (2\xi\omega + [\mathbf{\Phi}]^{\mathrm{T}}[\mathbf{C}^*]\,[\mathbf{\Phi}])\{\dot{\mathbf{x}}\} + \omega^2\{\mathbf{x}\} = [\mathbf{\Phi}]^{\mathrm{T}}\{\mathbf{F}\}. \tag{49}$$

The initial conditions on $\{\mathbf{x}\}$ can be obtained as follows:

$$\{\mathbf{x}_0\} = [\mathbf{\Phi}]^{\mathrm{T}}[\mathbf{M}]\{\bar{\mathbf{u}}_0\}, \qquad \{\dot{\mathbf{x}}_0\} = [\mathbf{\Phi}]^{\mathrm{T}}[\mathbf{M}]\{\dot{\bar{\mathbf{u}}}_0\}. \tag{50, 51}$$

4. NUMERICAL EXAMPLES

In this section, numerical examples are presented to verify the proposed finite element model. A cantilever composite beam with both the upper and lower surfaces symmetrically bonded by piezoelectric ceramics, as shown in Figure 1, is considered. The beam is made of T300/976 graphite/epoxy composites and the piezoceramic is PZT G1195N. The

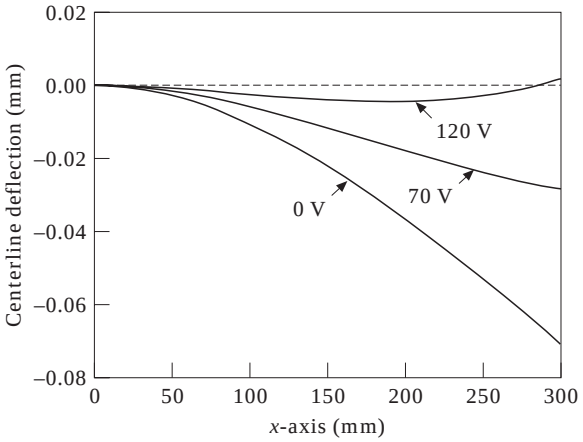

Figure 2. The centerline deflection of the cantilever composite beam with five pairs of actuators evenly distributed.

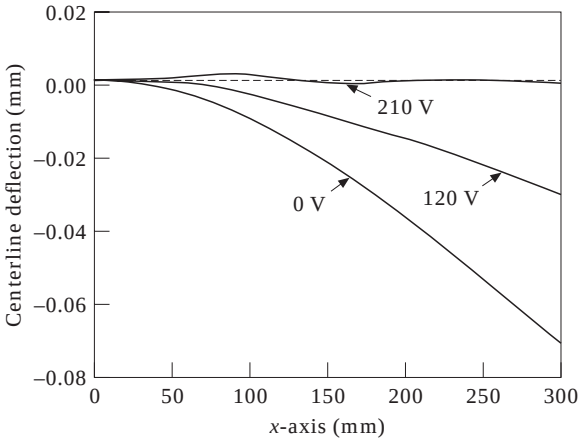

Figure 3. The centerline deflection of the cantilever composite beam with two pairs of actuators located at the left end and middle span of the beam.

adhesive layers are neglected. The material properties given in Table 1 are the same as those in reference [14]. The stacking sequence of the composite beam is $[-45^\circ/45^\circ]_s$. The total thickness of the composite beam is 9·6 mm and each layer has the same thickness (2·4 mm); and the thickness of each piezo-layer is 0·2 mm. The lower piezoceramics serve as sensors and the upper ones as actuators. The relative sensors and actuators form sensor/actuator (S/A) pairs through closed control loops. The control of the static deformation and the reduction of the free vibration of the beam under the distribution piezoelectric S/A pairs are studied.

4.1. SHAPE CONTROL

The composite beam is subjected to a steady concentrated force of 4 N at the free end. In the analysis, the beam is divided evenly into 30 elements. In the case of shape control, all the piezoceramics on the upper and lower surfaces of the beam are used as actuators. Equal-amplitude voltages with an opposite sign are applied to the upper and lower piezoelectric layers respectively to control the deformation of the composite beam subjected to the concentrated load. Due to the converse piezoelectric effect, the distributed

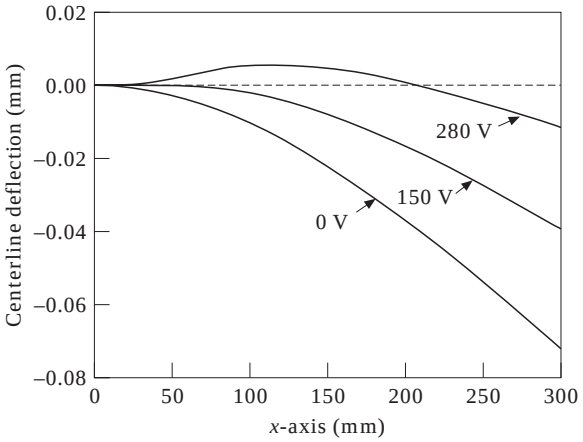

Figure 4. The centerline deflection of the cantilever composite beam with one pair of actuators located at the left end.

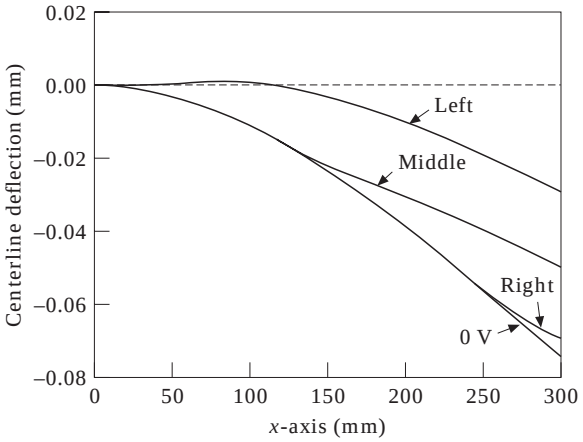

Figure 5. The centerline deflection of the cantilever composite beam with one pair of actuators at different position ($V = 200$ V).

piezoelectric actuators contract or expand depending on negative or positive active voltage. In general, for an upward displacement, the upper actuators need a negative voltage and the lower actuators need a positive one.

To investigate the effect of the number of actuator pairs on the deformation control, three sets of actuator pairs are considered: all the five pairs of actuators, two pairs (the left and the middle ones) and one pair (the left one). The calculated centerline deflections of the composite beam in the elevated environment with different pairs of actuators and different active voltages are shown in Figures 2–4. The comparison of the figures reflects the fact that a lower voltage is needed to eliminate the deflection caused by the external load when more actuators are used. It is shown in Figure 2 that the beam cannot be smoothly flattened with five pairs of actuators. When one pair of actuators is used, as shown in Figure 4, a very high active voltage is needed to quell the deformation and the beam is also not smoothly flattened. In Figure 3 it is shown that, under a certain active voltage, the beam can be flattened quite smoothly by two pairs of actuators. This fact indicates that, under some conditions, it is not appropriate to cover structures entirely with piezoelectrics from the view of efficiency and economy.

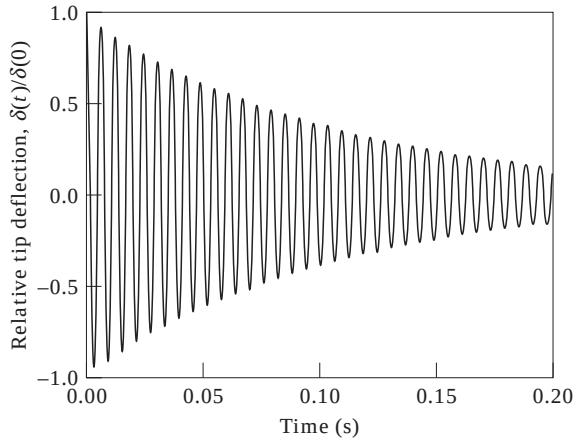

Figure 6. The effect of negative velocity gain on the cantilever composite beam subjected to first mode vibration (five pairs of S/As). Gain = 0 V/A.

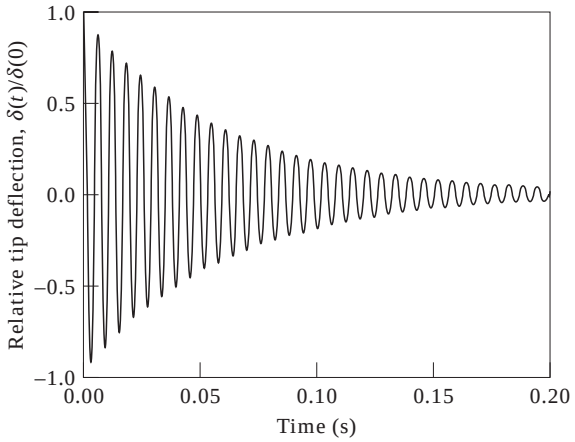

Figure 7. The effect of negative velocity gain on the cantilever composite beam subjected to first mode vibration (five pairs of S/As). Gain = −1·0E4 V/A.

The calculated centerline deflection of the composite beam with one pair of actuators at different positions is shown in Figure 5. A constant active voltage of 200 V with an opposite sign is applied on each actuator. The external force causing the mechanical deformation is the same as before. It is seen from Figure 5 that the location of the actuators has a significant effect on the control of the deformation. When the actuators are located at the free end of the cantilever beam (the right end), they are not useful in flattening the deformation. It is also clearly shown in Figure 5 that the actuators have a greater effect on flattening the deformation when the located position is closer to the fixed end (the left end). The actuators have the greatest effect when they are located on the fixed end. Compared to the effect of the number of actuators on the control of the deformation, the location of actuators plays a much more important role.

4.2. ACTIVE VIBRATION SUPPRESSION

The same piezoelectric composite beam given in Figure 1 is considered again to simulate the active vibration suppression through a simple S/A active control algorithm (negative velocity feedback). It is assumed that the cantilever beam is vibrating freely due to an initial

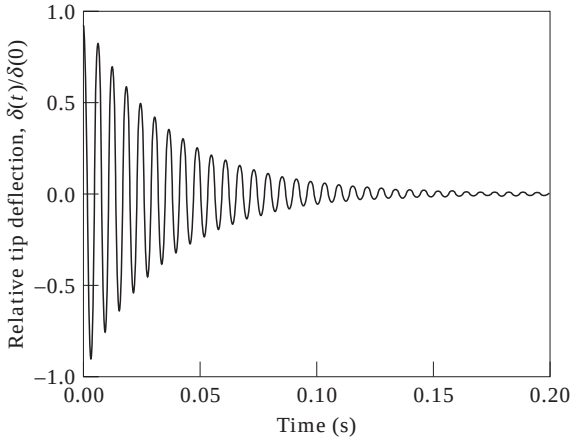

Figure 8. The effect of negative velocity gain on the cantilever composite beam subjected to first mode vibration (five pairs of S/As). Gain = −2·5E4 V/A.

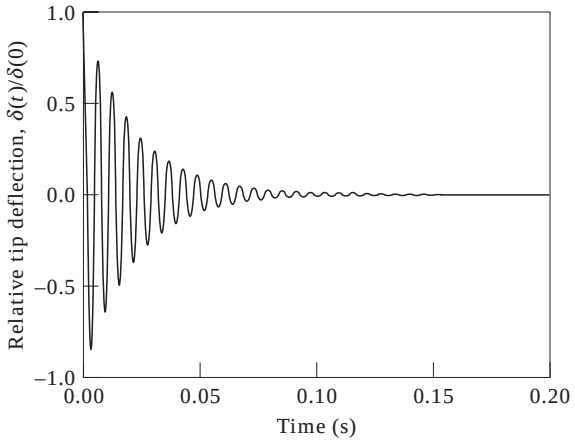

Figure 9. The effect of negative velocity gain on the cantilever composite beam subjected to first mode vibration (five pairs of S/As). Gain = −5·0E4 V/A.

disturbance (first mode) of $\delta(0)$ at the free end. The piezoceramics on the lower surface serve as sensors, and those on the upper surface are chosen as actuators. In the analysis, the whole beam is evenly divided into 30 elements, and each S/A pair covers six elements.

First, the modal superposition technique is used to decrease the size of the problem. The first six modes are used in the modal space analysis and an initial modal damping ratio for each of the modes is assumed to be 0·9%. Second, the transient response of the cantilever beam is computed by the Newmark direct integration method. The parameters γ and β are taken as one-half and one-quarter respectively.

In Figures 6–9 are shown the effects of negative velocity feedback control gains on the transient response of the cantilever composite beam subjected to the first mode vibration. Five S/A pairs are used in the vibration suppression. As shown in the figures, the vibrations decay more quickly when higher control gains are applied. However, it must be noted that the gains should be limited for the sake of the breakdown voltage of the piezoelectrics.

Similar to the shape control simulation, three sets of S/A pairs are considered in order to evaluate the effect of the number of S/As on the active vibration suppression: all the five pairs of S/As, two pairs (the left and the middle ones) and one pair (the left one). The

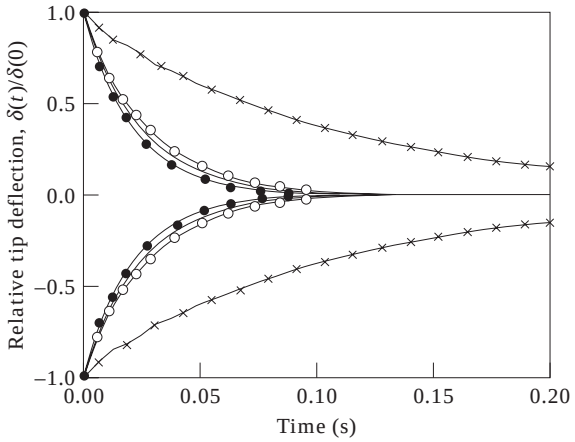

Figure 10. Decay envelopes of the tip displacement $\delta(t)$ for the cantilever composite beam with different pairs of S/As (Gain = −5·0E4 V/A). −×−, Uncontrolled; —●—, five pairs; —, two pairs; −○−, one pair.

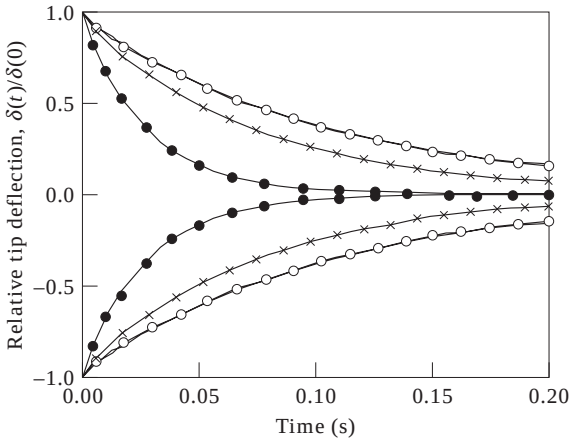

Figure 11. Decay envelopes of the tip displacement $\delta(t)$ for the cantilever composite beam with one pair of S/As at different positions (gain = −5·0E4 V/A). —, Uncontrolled; —●—, left; −×−, middle; −○−, right.

decay envelopes of the tip displacements for the cantilever beams with different pairs of S/As are shown in Figure 10. The control gain is $-5{\cdot}0 \times 10^4$ V/A for all three sets of S/As. The comparison shows that the vibrations are damped out more quickly with more S/A pairs. However, compared with the previous simulation, the effect of the number of S/As on the active vibration suppression is not as significant as on the shape control.

In Figure 11 are shown the decay envelopes of the tip displacements for the cantilever beams with one pair of S/A at different locations: at the right, the middle and at the left positions. The control gain is $-5{\cdot}0 \times 10^4$ V/A for the three different locations. It is seen that the position of S/A pairs is very important in vibration control: when the S/A is located at the free end (the right end), it is nearly useless in vibration suppression; on the contrary, the S/A pair has the best effect on vibration suppression when it is located at the fixed end. It can be concluded theoretically from the direct piezoelectric equation and practically from the comparison that the S/A pairs should be placed in regions of high average strains and away from areas of low strains. As for the vibration control of cantilever beams, for maximum effectiveness, the S/A pairs should be located as near to the fixed end as possible.

5. CONCLUSIONS

Based on third order laminate theory, an efficient and accurate finite element model for the active vibration control of laminated composite beams containing distributed piezoelectric S/As is developed. The negative velocity feedback control algorithm is used in the model to couple the direct and converse piezoelectric effects. The shape control and vibration suppression of a cantilever composite beam are investigated by using the model. The investigation shows that in designing smart structures with distributed piezoelectric S/As, the number and location of the S/As must be considered carefully. Two important points are revealed as follows:

(i) The positions of S/As have a critical influence on both the shape control and the vibration suppression of smart structures. For maximum effectiveness, the S/A pairs must be placed in high strain regions and away from areas of low strains.

(ii) The number of S/As has a great effect on the performance of smart structures. More S/As can usually induce greater efficiency on both the shape control and vibration suppression.

REFERENCES

1. T. Bailey and J. E. Hubbard 1985 *Journal of Guidance, Control, and Dynamics* **8**, 605–611. Distributed piezoelectric–polymer active control of a cantilever beam.
2. E. F. Crawley and J. de Luis 1987 *American Institute of Aeronautics and Astronautics Journal* **25**, 1373–1385. Use of piezoelectric actuators as elements of intelligent structures.
3. S. Im and S. N. Atluri 1989 *American Institute of Aeronautics and Astronautics Journal* **27**, 1801–1807. Effects of piezoactuator on a finitely deformed beam subjected to general loading.
4. J. N. Reddy 1984 *Journal of Applied Mechanics* **51**, 745–752. A simple higher-order theory for laminated composite plates.
5. N. D. Phan and J. N. Reddy 1985 *International Journal for Numerical Methods in Engineering* **21**, 2201–2219. Analysis of laminated composite plates using a higher-order shear deformation theory.
6. P. R. Heyliger and J. N. Reddy 1988 *Journal of Sound and Vibration* **126**, 309–326. A higher order beam finite element for bending and vibration problem.
7. C. K. Lee 1992 *Intelligent Structural Systems*. Dordrecht: Kluwer Academic. See pp. 75–167. Piezoelectric laminates: theory and experiment for distributed sensors and actuators.
8. P. F. Pai, A. H. Nayfeh, K. Oh and D. T. Mook 1993 *International Journal of Solids and Structures* **30**, 1603–1630. A refined nonlinear model of composite plates with integrated piezoelectric actuators and sensors.
9. D. K. Shah, W. S. Chan and S. P. Joshi 1993 *Proceedings of the AIAA/ASME/ASCE/AHS/ASC* 34*th Structures, Structural Dynamics, and Material Conference*, Part 6, 3189–3197. Finite element analysis of plates with piezoelectric layers.
10. I. Y. Shen 1995 *Smart Materials and Structures* **4**, 340–355. Bending and torsional vibration control of composite beams through intelligent constrained-layer damping treatments.
11. G. Shi and S. N. Atluri 1990 *Computers & Structures* **34**, 549–564. Active control of nonlinear dynamic response of space-frames using piezoelectric actuators.
12. H. S. Tzou 1989 *Journal of Robotics Systems* **6**, 745–767. Integrated distributed sensing and active vibration suppression of flexible manipulators using distributed piezoelectrics.
13. H. S. Tzou and C. I. Tseng 1990 *Journal of Sound and Vibration* **138**, 17–34. Distributed piezoelectric sensor/actuator design for dynamic measurement/control of distributed parameter system: a piezoelectric finite element approach.
14. S. K. Ha, C. Keilers and F. K. Chang 1992 *American Institute of Aeronautics and Astronautics Journal* **30**, 772–780. Finite element analysis of composite structures containing distributed piezoceramic sensors and actuators.
15. W. S. Hwang and H. C. Park 1993 *American Institute of Aeronautics and Astronautics Journal* **31**, 930–937. Finite element modelling of piezoelectric sensors and actuators.
16. K. Chandrashekhara and A. N. Agarwal 1993 *Journal of Intelligent Material Systems and Structures* **4**, 496–508. Active vibration control of laminated composite plates using piezoelectric devices: a finite element approach.
17. K. Chandrashekhara and R. Tenneti 1995 *Smart Materials and Structures* **4**, 281–290. Thermally induced vibration suppression of laminated plates with piezoelectric sensors and actuators.
18. R. C. Shieh 1993 *Proceedings of the AIAA/ASME/ASCE/AHS/ASC* 34*th Structures, Structural Dynamics, and Material Conference*, Part 6, 3250–3260. Finite element formulation for dynamic response analysis of multi-axially active, 3-dimensional piezoelectric beam element structures.
19. H. F. Tiersten 1969 *Linear Piezoelectric Plate Vibrations*. New York: Plenum Press.
20. K. J. Bathe 1987 *Finite Element Procedures in Engineering Analysis*. Englewood Cliffs, New Jersey: Prentice-Hall.